Published in final edited form as:

J Immunol. 2007 February 01; 178(3): 1512–1522.

Dendritic Cell Immunization Route Determines Integrin Expression and Lymphoid and Nonlymphoid Tissue Distribution of CD8 T Cells[1]

Stacey L. Sheasley-O'Neill, **C. Colin Brinkman**, **Andrew R. Ferguson**, **Melanie C. Dispenza**[2], and **Victor H. Engelhard**[3]

Department of Microbiology and Carter Immunology Center, University of Virginia, Charlottesville, VA 22908

Abstract

Exogenous dendritic cells (bone marrow-derived dendritic cell (BMDC)) display restricted trafficking in vivo after injection into mice, but the route(s) by which they generate gut-homing effector cells is unclear. Mesenteric lymph nodes (LN) and spleen were differentially targeted by i.p. and i.v. administration of BMDC, respectively, whereas mediastinal LN were targeted by both routes. BMDC injected by either route activated $CD8^+$ T cells to up-regulate both $\alpha_4\beta_1$ and $\alpha_4\beta_7$ integrins. However, the lymphoid compartment in which activation occurred determined their expression kinetics, magnitude, and population distribution. Only T cells activated in mesenteric LN after i.p. immunization expressed high levels of $\alpha_4\beta_7$, which also correlated with localization to small intestine. These $\alpha_4\beta_7^{high}$ cells also redistributed to mediastinal LN in a manner sensitive to treatment with $\alpha_4\beta_7$ blocking Abs, but not to mucosal addressin cell adhesion molecule-1 blocking Abs. Our results demonstrate the importance of lymphoid compartment, as dictated by immunization route, in determining integrin expression on activated T cells and their distribution in lymphoid and nonlymphoid tissues.

Appropriately activated dendritic cells (DC)[4] are potent APC, and exogenously administered Ag-pulsed DC induce specific $CD8^+$ T cell responses against viral and tumor Ags (1–4). However, the cellular nature and migration properties of exogenous DC limit their distribution in lymphoid compartments in an injection route-dependent manner (3, 5–9), leading to regionally constrained immune responses (3, 5). Thus, in contrast to replicating viral or bacterial immunogens that distribute widely in the body, immunization with bone marrow-derived DC (BMDC) creates the possibility to study the time course and

[1]This work was supported by U.S. Public Health Service Grants CA78400, AI20963, and AI059996 (to V.H.E.). S.L.S.-O. was supported by Training Grant GM07627.

[3]Address correspondence and reprint requests to Dr. Victor H. Engelhard, Carter Immunology Center, University of Virginia, Box 801386, Charlottesville, VA 22908-1386. vhe@virginia.edu.

[2]Current address: College of Medicine, Pennsylvania State University, University Park, PA 16802.

Disclosures

The authors have no financial conflict of interest.

[4]Abbreviations used in this paper: DC, dendritic cell; BMDC, bone marrow-derived DC; HEV, high endothelial venule; intintermediate; LN, lymph node; MAdCAM-1, mucosal addressin cell adhesion molecule-1; MFI, mean fluorescence intensity.

characteristics of the immune response initiated in individual lymph nodes (LN) in exquisite detail.

Taking full advantage of this capability requires greater understanding of the properties of BMDC as immunogens. One issue is how to target BMDC and the resulting T cell responses to different lymphoid compartments. Exogenous DC injected by i.v. or s.c. routes traffic into spleen alone or spleen and draining peripheral LN, respectively (3, 5–9), and induce primary responses localized to these same compartments (3). Importantly, neither s.c. nor i.v. immunization leads to localization of BMDC or T cell responses to mesenteric LN. Thus, it is currently unclear how to deliver BMDC to induce activation of $CD8^+$ T cells in lymphoid compartments associated with robust immunity in the gut.

Even if appropriately targeted, a second issue is to what extent BMDC matured in vitro induce molecules that mediate tissue-specific homing of T cells. $CD8^+$ T cells activated in vitro with endogenous DC enriched from mesenteric LN and Peyer's patches up-regulate $\alpha_4\beta_7$ integrin and CCR9, which are associated with gut homing (10–13). Conversely, peripheral LN-derived DC induce E- and P-selectin ligands that are associated with homing to the skin (13–15). A single study demonstrated that semimature BMDC have a limited ability to induce homing receptor expression in vitro (14), whereas more robust expression was observed after in vivo immunization. However, it was not established whether this difference was due to BMDC maturation in vivo, or alternatively, by different LN microenvironments.

In this study, we examined the $CD8^+$ T cell response that develops in individual lymphoid compartments after immunization with fully mature, CD40L-activated BMDC by different routes. We used T cell adoptive transfer to detect early priming events and track the ensuing immune response with great precision over time and space. Up-regulation of α_4 integrin expression on activated T cells was evaluated, and the relative roles of the BMDC and the lymphoid microenvironment in imprinting integrin expression were determined. Our results demonstrate route-dependent differences in activated T cell distribution in peripheral tissues. They also establish that $\alpha_4\beta_7^{high}$ cells activated in mesenteric LN redistribute into mediastinal LN via an $\alpha_4\beta_7$-dependent, but mucosal addressin cell adhesion molecule-1 (MAdCAM-1)-independent, mechanism.

Materials and Methods

Animals

C57BL/6 and OT-1 $RAG1^{-/-}$ mice were obtained from Charles River Laboratories and Taconic Farms, respectively. C57BL/6 Thy-1.1 and B6.C-$H2^{bm1}$/ByJ (bm1) mice were obtained from The Jackson Laboratory. All animals were maintained in pathogen-free facilities at the University of Virginia. All protocols were approved by the Institutional Animal Care and Use Committee.

Adoptive transfer of OT-1 cells

Single-cell suspensions from spleen and pooled LN of OT-1 $RAG1^{-/-}$ mice were enriched for $CD8^+$ T cells by negative selection (StemCell Technologies). Preparations were

consistently 97–99% $CD8^+$ by flow cytometry. In some cases, cells were labeled with 4 μM CFSE (Molecular Probes) in PBS for 15 min at 37°C before injection. Unless otherwise stated, 4×10^6 cells were injected i.v. into the dorsal tail vein.

DC culture and immunizations

BMDC were generated, as previously described, with slight modifications (16). Briefly, bone marrow cells removed from mouse femurs and tibias were cultured for 7 days in the presence of GM-CSF and IL-4 (BD Bio-sciences), enriched for DC by negative selection (StemCell Technologies), and activated by culturing overnight with NIH-3T3 cells expressing CD40L (a gift from R. Lapoint, University of Montreal, Quebec, Canada). These activated BMDC were uniformly $CD70^{high}CD80^{high}CD86^{high}$ and $CD62L^{negative}$, and expressed IL-12 (our unpublished observations). Before injection, BMDC were pulsed with 10 μM $OVA_{257–264}$ for 1 h at 37°C in the presence of 10 μg/ml human β_2-microglobulin (Calbiochem). Mice were immunized with 100,000 BMDC in 200 μl either i.v. into the dorsal tail vein or i.p. into the peritoneal cavity 18–36 h after adoptive transfer of OT-1 cells.

Flow cytometric analysis of surface markers

Samples were incubated with purified anti-CD16/CD32 (eBioscience) to block FcRs, and adoptively transferred cells were identified by staining with anti-CD8α PerCP, anti-CD8α PerCP-Cy5.5 (BD Biosciences), anti-Thy1.2 APC, anti-CD3ε biotin (eBioscience), and/or H-$2K^b$-OVA_{257} tetramer-APC generated in house by S. Lewis (University of Virginia Cancer Center, Charlottesville, VA). T cell activation status was evaluated with anti-CD25 FITC and anti-CD44 PE (eBioscience). Integrin expression was evaluated using anti-$\alpha_4\beta_7$ PE, anti-α_4 PE, or anti-α_4 biotin, followed by streptavidin-PerCP (BD Biosciences). Expression after in vivo injection of anti-$\alpha_4\beta_7$ was detected using PE goat anti-rat IgG (Jackson ImmunoResearch Laboratories). Chemokine receptor expression was evaluated using anti-CCR9 PE (R&D Systems). Samples were collected on a FACSCalibur (BD Biosciences) and analyzed using Flow Jo software.

FTY720 treatment and in vivo Ab blockade

Mice were injected i.p. with 1 mg/kg FTY720 (a gift from V. Brinkmann, Novartis Pharma, Basel, Switzerland) in 200 μl beginning 24 h after BMDC immunization and then every 24 h until harvest. Purified anti-CD62L (MEL-14) (17) (American Type Culture Collection), anti-$\alpha_4\beta_7$ (DATK32) (18), anti-MAdCAM-1 (MECA367) (19) (both gifts from J. Rivera-Nieves, University of Virginia, Charlottesville, VA), or rat IgG (20) were administered i.v. at 100 μg per mouse. Anti-CD62L treatment was initiated 6 h after BMDC injection, and anti-$\alpha_4\beta_7$ and anti-MAdCAM-1 treatments were initiated 24 h after BMDC injection. Ab injections were repeated every 24 h until harvest.

Activation of OT-1 cells in vitro

CD8-enriched CFSE-labeled OT-1 cells were cultured in a 96-well U-bottom plate at a 1:1 or 1:2 ratio with either CD40L-activated, $OVA_{257–264}$-pulsed, or unpulsed BMDC, or endogenous DC from mediastinal LN and spleen of mice that had been treated with 10 μg of human *fms*-like tyrosine kinase-3 ligand (Amgen) daily for 10 days and enriched by

negative selection (StemCell Technologies). Wells were harvested after 4–6 days and stained for Thy1.2, CD8α, $\alpha_4\beta_7$, and/or α_4 expression.

Staining of LN high endothelial venules (HEV) by immunofluorescence

Mice were injected i.v. with 100 μg of anti-MAdCAM-1 (MECA367) or rat IgG. Thirty minutes after Ab injection, LN were resected and snap frozen. Acetone-fixed frozen sections of LN were incubated with Alexa594 goat anti-rat IgG (Molecular Probes) and FITC anti-smooth muscle α-actin (20). Images were captured on a Nikon TE-300 inverted microscope and Bio-Rad μ-Radiance confocal system.

Generation of bone marrow chimeras

Mice were irradiated (650 rad × 2) using a Gammacell 40 (Nordion International). Bone marrow cells from donor mice were depleted of T cells by incubation with biotinylated anti-CD4 and anti-CD8α (eBioscience), followed by negative selection (StemCell), and injected (2.5×10^6 in 200 μl) into the dorsal tail vein. Mice were used in experiments 10–14 wk after injection of donor bone marrow cells.

Lymphocyte recovery from peripheral tissues

Lymphocytes were recovered from lung by purging lungs of blood using a heparin solution, followed by digestion with 125 U/ml collagenase type XI, 60 U/ml DNase I, and 60 U/ml hyaluronidase type I-s (20), and lymphocytes were purified by centrifugation on a Histodenz gradient (20). Intraepithelial lymphocytes from the small intestine were isolated by excising from the duodenum to the cecum, removing Peyer's patches, digesting with 1 mM DTT (Roche Applied Science), and isolating lymphocytes on a Percoll gradient (20, 21). Intrahepatic lymphocytes were isolated by flushing the liver with 0.05% collagenase IV (20) before removal, digestion with 0.05% collagenase IV, and isolation of lymphocytes on a Histodenz-based gradient (22).

Statistical analyses

Statistical analyses were performed using two-way ANOVA (Sigma-Aldrich Stat software).

Results

BMDC administered i.p. and i.v. prime naive CD8$^+$ T cells in distinct lymphoid compartments

Previous studies had not established a route by which injected exogenous BMDC could infiltrate mesenteric LN and activate resident T cells. Consequently, we compared the localization of T cell activation after i.p. and i.v. injection of OVA_{257} peptide-pulsed CD40L-activated BMDC. To enhance detection of early activation events, CD8$^+$ OT-1 TCR transgenic T cells were adoptively transferred into mice 18–36 h before immunization. Twenty-two hours after immunization, OT-1 cells in different lymphoid organs were identified by staining with H2-K^b-OVA_{257} tetramer, and their activation status was determined based on up-regulation of CD25 (Fig. 1*a*). Activated OT-1 cells were present in mesenteric LN following i.p., but not i.v. injection of BMDC. Conversely, T cell activation

was observed in the spleen after i.v., but not i.p. injection. Whereas neither route of immunization led to activation of T cells in axillary/brachial LN, both led to T cell activation in mediastinal LN. These results were consistent in six independent experiments representing a total of 16 mice (Fig. 1*b*), and also using CD69 up-regulation as another early marker of activation (our unpublished observations). We also examined whether functional DC redistributed to additional lymphoid compartments with a delayed time course by injection of CFSE-labeled OT-1 cells into mice that had been immunized with BMDC 48 h previously. However, T cell activation at these later times remained localized to the same compartments, although the magnitude of activation waned somewhat by 48 h (Fig. 1*c*). These data demonstrate that activation of $CD8^+$ OT-1 cells by exogenous BMDC was localized to distinct lymphoid compartments after i.p. and i.v. injection, and that mesenteric LN were targeted only by the i.p. route.

Intraperitoneal but not i.v. immunization effectively generates gut-localized activated OT-1 cells

To determine whether the early activation of T cells in distinct lymphoid compartments led to a productive response, we examined the dilution of CFSE in labeled OT-1 cells 72 h after immunization. Activated OT-1 cells underwent substantial proliferation and expansion in all compartments in which up-regulation of CD25 on T cells had been observed (priming compartments) (Fig. 2*a*). Greater than 95% of OT-1 cells remained undivided in the same compartments of mice that had received either no BMDC or unpulsed BMDC (our unpublished observations). To evaluate whether activated OT-1 cells could localize to nonlymphoid tissues, peripheral tissues were harvested 6 days after immunization. At this time point, the percentages of OT-1 cells in spleen were similar after immunization by either route (Fig. 2*b*). In addition, substantial increases in OT-1 cells in lung and liver were evident after both i.p. and i.v. immunization. These cells were $CD44^{high}$ and $CD62L^-$, consistent with an effector T cell phenotype (Fig. 2*c*). Activated OT-1 cells were equally prevalent in each of these tissues regardless of the immunization route. In contrast, the percentage of activated OT-1 cells in the small intestine was >6-fold greater after i.p. than i.v. immunization. Thus, only i.p. immunization effectively generated gut-resident OT-1 cells.

Both routes of immunization generate $\alpha_4\beta_7^+$ -activated OT-1 cells, but the level of $\alpha_4\beta_7$ expressed is route dependent

Because of the known role of $\alpha_4\beta_7$ integrin expression in homing of T cells to the gut, the expression of α_4 integrins on activated OT-1 cells in priming compartments was evaluated. After i.p. immunization, divided OT-1 cells in both mesenteric and mediastinal LN gradually up-regulated α_4 integrin expression, becoming nearly 100% α_4^+ by the sixth division (Fig. 3*a*). The majority of cells in mesenteric LN also up-regulated $\alpha_4\beta_7$ expression by the sixth division. However, $\alpha_4\beta_7$ expression was delayed relative to that of α_4 by ~2 cell divisions (Fig. 3*b*). Because α_4 only heterodimerizes with β_1 and β_7, this observation indicates that these cells up-regulated $\alpha_4\beta_1$ first. Interestingly, α_4 expression on cells in mediastinal LN was delayed relative to that on cells in mesenteric LN by ~2 cell divisions (Fig. 3*b*). Also, whereas most activated cells in mediastinal LN after i.p. immunization expressed $\alpha_4\beta_1$, a significant fraction was $\alpha_4\beta_7^+$ (Fig. 3*a*). Following i.v. immunization, divided OT-1 cells in the mediastinal LN and spleen also became nearly 100% α_4^+ by the sixth division (Fig. 3, *c*

and *d*). The majority of these cells failed to express $\alpha_4\beta_7$; thus, the dominant population that developed in both lymphoid compartments was $\alpha_4\beta_1^+$. Unexpectedly, however, a small, but reproducible proportion of cells activated in both spleen and mediastinal LN became $\alpha_4\beta_7^+$. Activated cells with a similar distribution of α_4 integrins were also evident in mesenteric LN (Fig. 3, *c* and *e*). This is consistent with the earlier demonstration that the mesenteric LN was not a priming site after i.v. immunization, and that it is not the source of the $\alpha_4\beta_7^+$ cells observed. Collectively, these results establish that the kinetics and relative expression of $\alpha_4\beta_1$ and $\alpha_4\beta_7$ integrins after BMDC immunization were lymphoid compartment dependent.

The above results suggested that the presence of gut-resident OT-1 cells after i.p. immunization was correlated with a dominant population of $\alpha_4\beta_7^+$ cells in mesenteric LN, which is in keeping with previous work from many laboratories. Indeed, the entry of these cells into the gut was blocked by in vivo administration of Abs against either $\alpha_4\beta_7$ or its ligand, MAdCAM-1 (see Fig. 4*i*). However, significant numbers of divided $\alpha_4\beta_7^+$ OT-1 cells were also found in other priming compartments after both i.p. and i.v. immunization. A possible explanation for the route-dependent difference in localization of OT-1 cells to gut is that i.p. immunization generated larger numbers of $\alpha_4\beta_7^+$ cells. However, despite the greater proportion of $\alpha_4\beta_7^+$ OT-1 cells generated in mesenteric LN after i.p. immunization, the absolute number of $\alpha_4\beta_7^+$ cells generated after i.v. immunization was 2- to 3-fold greater because the spleen contained 10–15 times as many OT-1 cells as the mesenteric LN (our unpublished observations). This indicated that the paucity of activated OT-1 cells in gut after i.v. immunization was not due to lower absolute numbers of $\alpha_4\beta_7^+$ cells generated. However, we also noted that the level of $\alpha_4\beta_7$ expression on extensively divided OT-1 cells was route dependent. Whereas T cells activated after i.v. immunization expressed intermediate levels of $\alpha_4\beta_7$ ($\alpha_4\beta_7^{int}$) (Fig. 3*e*), those in i.p. immunized animals expressed ~2.3 times more ($\alpha_4\beta_7^{high}$) (Fig. 3*f*) based on mean fluorescence intensity (MFI) (23). The MFI of $\alpha_4\beta_7^+$ cells in the mediastinal LN varied in different experiments based on staining conditions, and was in some cases lower than that of cells in mesenteric LN (see Figs. 5 and 6). However, it was always higher than that of cells isolated from the mediastinal LN of mice immunized by the i.v. route in the same experiment. Additionally, cells expressing intermediate levels of $\alpha_4\beta_7$ were found in the mesenteric LN after i.v. immunization. This suggests that the level of $\alpha_4\beta_7$ integrin either directly determines the ability to home to the gut, or serves as a phenotypic marker for expression of other molecules that do so. To examine the latter possibility, the expression of CCR9 was examined due to the involvement of this receptor in migration of cells to the gut. Cells that had divided and expressed $\alpha_4\beta_7$ in the mesenteric LN after i.p. BMDC immunization expressed CCR9. Conversely, divided cells expressing $\alpha_4\beta_7$ in the mediastinal LN after i.v. BMDC immunization did not express CCR9 over levels found on undivided cells in a mouse receiving no BMDCs (Fig. 3*g*). This reveals two different $\alpha_4\beta_7^+$ populations that arise in different lymphoid organs.

The $\alpha_4\beta_7^{high}$ subpopulation present in mediastinal LN following i.p. immunization originates in mesenteric LN

To investigate the basis for immunization route-dependent differences in $\alpha_4\beta_7^+$ populations in mediastinal LN, we first tested the hypothesis that this difference was due to T cell

activation in distinct LN within the mediastinum after i.v. and i.p. immunization. The mediastinal LN used in our experiments were collected from the anterior and posterior mediastinum (also known as parathymic and paratracheal LN, respectively). Therefore, T cell activation was evaluated separately in parathymic and paratracheal LN 22 h after BMDC injection. Following i.p. administration, OT-1 cells in both LN were activated, although the fraction activated in parathymic LN was consistently higher (Fig. 4*a*). However, after i.v. injection, OT-1 cell activation was almost completely confined to the paratracheal LN. This suggested that BMDC injected into the peritoneal cavity accessed afferent lymphatics of parathymic LN, whereas BMDC present in lung after i.v. injection could not. In contrast, afferent lymphatics of the paratracheal LN were accessed by BMDC draining from both the lungs and peritoneal cavity. Whereas these results were consistent with the hypothesis that differential mediastinal priming after i.p. and i.v. immunization might lead to different $\alpha_4\beta_7$ expression levels, the levels of $\alpha_4\beta_7$ on extensively divided cells in parathymic and paratracheal LN were similar 3 days after i.p. immunization (Fig. 4*b*). Thus, despite the activation of T cells in different mediastinal LN after i.v. and i.p. immunization, this did not account for differences in the expression of $\alpha_4\beta_7$ because when activation occurred in both mediastinal compartments, $\alpha_4\beta_7$ expression levels on cells in those compartments were equivalent to each other.

We next tested an alternate hypothesis that $\alpha_4\beta_7^{high}$ OT-1 cells were generated in mesenteric LN and subsequently recirculated into mediastinal LN. To do this, we treated animals with FTY720, a drug that inhibits lymphocyte egress from LN (24), to sequester T cells in the compartments in which they were activated. In i.p. immunized mice treated with FTY720, the MFI of extensively divided $\alpha_4\beta_7^+$ cells in mediastinal LN was only about half that of the $\alpha_4\beta_7^+$ population in mesenteric LN of the same animal (Fig. 4*c*), and was similar to what was observed in mediastinal LN and spleen after i.v. immunization. Additionally, the percentage of $\alpha_4\beta_7^+$ cells in mediastinal LN of FTY720-treated mice was significantly reduced, whereas there was no effect on cells in the mesenteric LN (Fig. 4*d*). These data demonstrated that the subpopulation of $\alpha_4\beta_7^{high}$ OT-1 cells in mediastinal LN after i.p. immunization resulted from the redistribution of cells activated in mesenteric LN.

Entry of $\alpha_4\beta_7^{high}$ OT-1 cells in mediastinal LN is not mediated by CD62L, but is $\alpha_4\beta_7$ dependent

The redistribution of activated $\alpha_4\beta_7^{high}$ T cells from mesenteric to mediastinal LN was unexpected. Because CD62L expression on naive T cells mediates entry into LN, we used in vivo blockade with anti-CD62L Ab (25) to test the hypothesis that entry of $\alpha_4\beta_7^{high}$ cells into mediastinal LN would also be mediated by this selectin. As expected, the cellularity of the peripheral LN in mice treated with anti-CD62L for 66 h was substantially reduced, whereas the cellularity of the spleen was slightly increased (our unpublished observations). However, the MFIs of extensively divided $\alpha_4\beta_7^+$ cells in mesenteric and mediastinal LN were not significantly diminished in i.p. immunized mice treated with anti-CD62L compared with those treated with rat IgG as a control (Fig. 5*a*). Additionally, there was no diminution in the percentage of $\alpha_4\beta_7^+$ cells as a function of cell division number (Fig. 5*b*). Together, these data indicated that entry of $\alpha_4\beta_7^{high}$ cells into mediastinal LN was CD62L independent.

We next used in vivo blockade with anti-$\alpha_4\beta_7$ (25) to evaluate whether entry of $\alpha_4\beta_7^{high}$ cells into mediastinal LN was mediated by this integrin. Because $\alpha_4\beta_7$ blockade was achieved with the same Ab used for staining ex vivo, PE-conjugated anti-rat IgG was used to detect $\alpha_4\beta_7^+$ cells that had bound Ab in vivo. This increased the MFI of all $\alpha_4\beta_7^+$ cells isolated from these animals, regardless of compartment, relative to the MFI of cells isolated from mice treated with rat IgG and stained directly (Fig. 5*c*). Despite this, the percentages of $\alpha_4\beta_7^+$ cells detected in mesenteric LN of i.p. immunized mice that had been treated with either anti-$\alpha_4\beta_7$ or rat IgG were comparable (Fig. 5*d*). The percentages of these cells that had migrated through the circulation to spleen at this time were also comparable. However, anti-$\alpha_4\beta_7$ blockade substantially reduced the percentage of divided $\alpha_4\beta_7^{high}$ cells in both parathymic and paratracheal LN of i.p. immunized mice. This effect was limited to these LN, and there was no impact on the percentage of $\alpha_4\beta_7^+$ in the spleen. In the experiment shown, the MFI of extensively divided $\alpha_4\beta_7^+$ OT-1 cells in parathymic and paratracheal LN of rat IgG-treated mice was only ~65–80% of the MFI of cells from mesenteric LN and spleen. However, in anti-$\alpha_4\beta_7$-treated mice, the MFI of cells from parathymic and paratracheal LN was reduced to only ~30% of that in mesenteric LN of the same animal, whereas the relative MFI of cells in the spleen remained at 90% (Fig. 5*c*). We attribute the somewhat lower MFI of cells from parathymic and paratracheal LN of rat IgG-treated mice to somewhat lower infiltration of $\alpha_4\beta_7^{high}$ cells relative to $\alpha_4\beta_7^{int}$ cells activated in the same compartment. The selective reduction in both the MFI and the percentage $\alpha_4\beta_7^+$ cells in parathymic and paratracheal LN was observed in four independent experiments. These results demonstrate that entry of $\alpha_4\beta_7^{high}$ cells into both components of the mediastinal LN is mediated by $\alpha_4\beta_7$ itself.

MAdCAM-1 is expressed on HEV in parathymic and paratracheal LN, but entry of $\alpha_4\beta_7^{high}$ OT-1 cells into mediastinal LN is not MAdCAM-1 dependent

It has been established that the major ligand for $\alpha_4\beta_7$ enabling entry into small intestine and its associated lymphoid tissue is mucosal vascular addressin MAdCAM-1 (25). However, its expression in mediastinal LN has not been reported. When we examined parathymic and paratracheal LN in naive and i.p. immunized animals by immunofluorescence, MAdCAM-1 expression was observed on HEV (as identified by costaining with anti-smooth muscle α-actin) (Fig. 6, *a*–*e*). By comparison with mesenteric LN, this expression was limited to a subset of HEV. To test the hypothesis that this ligand was binding $\alpha_4\beta_7$ on OT-1 cells to allow entry into mediastinal LN, i.p. immunized mice were treated with anti-MAdCAM-1 Ab (19). Surprisingly, MAdCAM-1 blockade had no effect on the presence of $\alpha_4\beta_7^{high}$ cells in either component of the mediastinal LN, based either on a reduction in the MFI of extensively divided $\alpha_4\beta_7^{high}$ cells in treated mice relative to their rat IgG-treated counterparts (Fig. 6*f*), or the percentage of $\alpha_4\beta_7^+$ cells (Fig. 6*g*). In contrast, MAdCAM-1 blockade almost completely inhibited entry of activated OT-1 cells into small intestine (Fig. 6*i*). In total, these data demonstrated that despite expression of MAdCAM-1 on HEV, entry of $\alpha_4\beta_7^{high}$ cells into mediastinal LN was MAdCAM-1 independent.

Ag-presenting BMDC require the lymphoid microenvironment to induce $\alpha_4\beta_7$, but not $\alpha_4\beta_1$ up-regulation on activated T cells

The results of Figs. 3 and 4 established that the kinetics, level, and type of α_4 integrin expression induced by immunization with exogenous BMDC varied with the lymphoid compartment in which activation occurred. Therefore, we examined the relative contributions of the BMDC themselves and the lymphoid microenvironment in imprinting α_4 integrin expression. To assess the ability of BMDC to induce $\alpha_4\beta_1$ and $\alpha_4\beta_7$ expression on activated T cells in the absence of the lymphoid microenvironment, OT-1 cells were stimulated with OVA_{257}-pulsed CD40L-activated BMDC in vitro. Divided OT-1 cells did not express $\alpha_4\beta_7$ after 4 days (Fig. 7*a*) and remained $\alpha_4\beta_7^{negative}$ after 6 days (our unpublished observations), indicating that the lymphoid microenvironment was necessary for imprinting both $\alpha_4\beta_7^{int}$ and $\alpha_4\beta_7^{high}$ expression. In contrast, virtually all of these cells became $\alpha_4\beta_1^{+}$ by the second cell division. Interestingly, peptide-pulsed endogenous DC enriched from mediastinal LN or spleen did not significantly increase $\alpha_4\beta_1$ expression on OT-1 cells during activation in vitro, despite inducing robust proliferation (Fig. 7*b*). This indicates that the simple acquisition of $\alpha_4\beta_1$ on activated CD8 T cells is a property of exogenous BMDC and not of the lymphoid microenvironment.

Several studies have demonstrated that DC enriched from mesenteric LN can imprint $\alpha_4\beta_7$ expression on T cells during activation in vitro (10–12). Because BMDC were unable to up-regulate $\alpha_4\beta_7$, this raised the question of whether the endogenous cells in the LN that imprinted expression of this integrin in vivo also were responsible for presenting Ag. To address this, we used irradiated C57BL/6 mice reconstituted with bone marrow from bm1 mice, which have a mutated H-$2K^b$ molecule that is unable to present OVA_{257} to OT-1 cells (26). After i.p. immunization with OVA_{257}-pulsed BMDC derived from B6 mice, OT-1 cells in both bm1 and B6 bone marrow chimeras showed comparable overall activation based on CFSE dilution profiles (Fig. 7*c*). Importantly, $\alpha_4\beta_7$ expression occurred with similar kinetics and expression levels in both chimeras (Fig. 7, *d* and *e*). This same result was also observed by ablation of endogenous Ag presentation using β_2-microglobulin-deficient mice (our unpublished observations). These results demonstrated that $\alpha_4\beta_7$ integrin expression after BMDC immunization did not require Ag presentation by endogenous DC. Interestingly, we found that the delayed kinetics of $\alpha_4\beta_1$ up-regulation in mediastinal LN as compared with mesenteric LN (previously shown in Fig. 3*b*) was also observed in i.p. immunized bm1 chimeras (Fig. 7, *f* and *g*). These results establish that the induction of $\alpha_4\beta_7$ expression and modulation of $\alpha_4\beta_1$ expression kinetics on T cells activated by BMDC are properties of the lymphoid microenvironment, and are separable from the cells in LN that present Ag.

Discussion

In this study, we have used BMDC to gain insight into the activation of $CD8^+$ T cells occurring in individual lymphoid compartments. BMDC introduced by different routes entered distinct lymphoid compartments, enabling us to compare T cell responses in these specific environments. By using preactivated, peptide-pulsed BMDC that traffic rapidly, we avoid the more prolonged accumulation of cells presenting Ag, as well as their uncertainty about their distribution, which would occur using virus or peptide in adjuvant. This enabled

us to evaluate the kinetics of T cell activation and differentiation with a high degree of precision. Activated OT-1 cells in all priming compartments up-regulated $\alpha_4\beta_1$ integrin. This was mediated by BMDC, although the lymphoid microenvironment impacted the kinetics of up-regulation. In contrast, $\alpha_4\beta_7$ expression was imprinted by the lymphoid microenvironment, but endogenous Ag presentation was not required. The microenvironment controlled not only the proportion of cells that ultimately expressed this integrin, but also its level on individual cells. Only those cells expressing high levels of $\alpha_4\beta_7$ after activation in mesenteric LN were able to home to the gut. These same cells redistributed into both parathymic and paratracheal LN early after activation by an $\alpha_4\beta_7$-dependent, but MAdCAM-1- and CD62L-independent mechanism. These results identify distinct roles for BMDC and the lymphoid microenvironment in determining integrin expression on activated T cells and the redistribution of these cells into both lymphoid and nonlymphoid tissues.

Our work offers new insights into the precise sites of BMDC trafficking after introduction by different routes. Whereas prior work established localization of BMDC to spleen following i.v. introduction (3, 5–9), their entry into paratracheal LN has not been reported. This observation, however, is consistent with the involvement of the paratracheal LN as the major receptacle of lung lymphatic drainage (27), and the entry of BMDC into lung shortly after i.v. introduction (5, 6, 9, 27, 28). In contrast, there have been significant discrepancies among studies evaluating cell migration out of the peritoneal cavity. Lymphocytes introduced i.p. migrated to mediastinal, but not mesenteric LN (29). Conversely, another study that used indium-111-labeled BMDC found migration only to the spleen (6). However, the association of radioactivity with viable and functional BMDC was not established. In this study, we have demonstrated that Ag-presenting BMDC introduced i.p. trafficked to mesenteric LN and both parathymic and paratracheal LN. Whereas BMDC may have specific migratory capacities to access mesenteric LN that lymphocytes lack, we found no evidence for delayed entry of functional BMDC into any other lymphoid compartment after either i.p. or i.v. introduction, even after waiting up to 48 h. Because only targeting of mesenteric LN led to gut-localized effectors, these data suggest that i.p., but not i.v. immunization would be likely to provide protection against infection or tumor in the gut.

The use of BMDC as immunogens allowed us to follow the process of T cell activation in individual LN with a new level of precision, and to establish that the details are different in distinct lymphoid compartments. Whereas the expression of $\alpha_4\beta_7$ integrin by a majority of T cells activated within mesenteric LN is consistent with earlier studies (11, 30), our work demonstrates that it is also expressed at lower levels on small, but significant populations of cells activated in other compartments. These $\alpha_4\beta_7^{int}$ cells do not express CCR9 and do not home to the gut, and their functional significance remains to be investigated. In addition, the expression of $\alpha_4\beta_7$ on cells activated in mesenteric LN was significantly delayed relative to that of $\alpha_4\beta_1$. Because we have established that BMDC suffice to induce $\alpha_4\beta_1$, whereas $\alpha_4\beta_7$ is controlled by the microenvironment, these results suggest that the microenvironmental influence is delayed, and that it operates to control expression of β_7. Although it is not clear whether these cells continue to express $\alpha_4\beta_1$, they do remain β_1 positive (our unpublished observations). Thus, the use of BMDC has illuminated details of the T cell differentiation process in mesenteric LN that were not previously appreciated. Finally, we have

demonstrated that the kinetics of $\alpha_4\beta_1$ expression as a function of cell division were delayed in mediastinal LN as compared with mesenteric LN. This might reflect the influence of microenvironmental factors that promote or delay expression that is induced by BMDC. Alternatively, it may result from differences in BMDC number or kinetics of infiltration in different lymphoid compartments. Regardless of the mechanism, the results establish both qualitative and quantitative differences in the differentiation of activated T cells in individual LN.

One hypothesis to explain these compartmental differences is that they reflected the entry of distinct functional subsets of BMDC that developed under the influence of the nonlymphoid environment at the site of injection. Indeed, Calzascia et al. (31) concluded that α_4 integrin and E- and P-selectin ligand expression on activated T cells in different LN was determined by the site from which DC trafficked, and not the LN microenvironment. However, we found that α_4 integrin expression of T cells activated in mediastinal LN after i.v. and i.p. immunization was the same, despite BMDC entry via different lymphatics. In addition, BMDC injected into the peritoneal cavity generated predominantly $\alpha_4\beta_7^{high}$ cells in mesenteric LN, but predominantly $\alpha_4\beta_1^{+}$ cells in mediastinal LN. Thus, different T cell differentiation programs were induced in distinct lymphoid compartments infiltrated by BMDC from the same source. One important difference is that Calzascia et al. (31) used locally injected tumor to introduce Ag into resident DC in different peripheral compartments, rather than the exogenous BMDC used in this study. These BMDC are uniformly highly activated, with no evidence of functional heterogeneity, and are not likely to be susceptible to further maturation under the influence of the injection environment. Whereas we cannot rule out peripheral tissue-dependent differences in DC maturation, our data clearly point to an important role of the lymphoid environment in determining the kinetics and extent to which T cells acquire integrin expression that is independent of this possibility.

This conclusion is in keeping with the demonstration that resident DC from different LN compartments imprint homing receptor expression on T cells (13, 32), and the identification of retinoic acid as a soluble mediator of $\alpha_4\beta_7$ imprinting (33). It is also in keeping with the demonstration that $\alpha_4\beta_7$ expression on circulating effectors was much higher after BMDC immunization in vivo than after in vitro culture (14). Because the BMDC used were immature, this was interpreted to reflect their maturation in vivo. Conversely, we have demonstrated in this study that whereas CD40L-activated, peptide-pulsed BMDC were unable to induce $\alpha_4\beta_7$ expression in vitro, its induction in vivo was not dependent on Ag presentation by endogenous DC. Thus, our data demonstrate that Ag presentation and induction of $\alpha_4\beta_7$ expression need not be mediated by the same cell in the LN.

A final important observation in this work was that $\alpha_4\beta_7^{high}$ T cells rapidly redistributed into mediastinal LN from their site of activation in mesenteric LN. The redistribution of activated T cells is not readily apparent when examining immune responses to systemically distributing virus or peptide because of the inability to distinguish cells that were primed in a compartment from cells recirculating into that compartment. In a small number of studies using localized Ag challenge (34, 35), redistribution to noncontiguous LN was inferred from the extent of cell division of Ag-specific cells, but more extensive Ag presentation in these

additional compartments due to Ag spreading was not excluded. The use of localized BMDC immunization and FTY720 to block T cell egress from LN definitively demonstrates the existence of this LN to LN redistribution process. We have characterized this process in greater detail elsewhere (S. Sheasley-O'Neill, C. C. Brinkman, and V. H. Engelhard, manuscript submitted). This work has demonstrated that redistribution is widespread in different LN compartments and usually mediated by CD62L. However, in the present work, we have made the novel observation that the entry of these cells into mediastinal LN is mediated by $\alpha_4\beta_7$, not CD62L, but apparently via recognition of a ligand other than MAdCAM-1. This is surprising because MAdCAM-1 is the major ligand for $\alpha_4\beta_7$-mediated entry into gut and GALT (25), and we found it on a subset of mediastinal LN HEV. However, MAdCAM-1 is also expressed in the sinus-lining cells of the spleen, but is irrelevant for homing to that organ (36, 37). We considered the possibility that $\alpha_4\beta_7^{high}$ cells enter mediastinal LN via afferent lymphatics from lung or peritoneal cavity rather than from the bloodstream. However, this is unlikely because we have shown that entry into mediastinal LN is blocked using anti-$\alpha_4\beta_7$ Ab in vivo, whereas this maneuver has no effect on lymphocyte entry into lung (25). Additionally, lymphocyte entry into the peritoneal cavity has been shown to be dependent on P- or E-selectin ligands (38, 39). Together, this suggests that entry of activated $\alpha_4\beta_7^{high}$ cells is mediated by $\alpha_4\beta_7$ integrin binding to an as yet unidentified ligand expressed on mediastinal LN HEV.

In summary, this study demonstrates that BMDC immunization route determines the sites of T cell priming, which then impacts integrin expression on activated T cells and the distribution of activated cells in lymphoid and nonlymphoid tissues. This work has important clinical implications because BMDC-based immunotherapeutic strategies to date have not specifically addressed the route of immunization as a variable, nor considered the possibility that routing might alter the ability to generate gut-associated immunity. These results underscore the importance of site of BMDC targeting in inducing differentially targeted immune responses, and provide insight into mechanisms of homing receptor imprinting resulting from BMDC immunization.

Acknowledgments

We thank Janet V. Gorman and Sarah T. Lewis for excellent technical assistance. We also thank Dr. Victoria Camerini, Dr. Young Hahn, and Dr. Thomas Braciale for providing the lymphocyte recovery protocols for the small intestine, liver, and lung, respectively. We thank T. J. O'Neill for assistance with the analysis of LN HEV by immunofluorescence. Finally, we thank Dr. Klaus Ley, Dr. Timothy Bullock, and Lisa Nichols for their insightful discussions.

References

1. Inaba K, Metlay JP, Crowley MT, Steinman RM. Dendritic cells pulsed with protein antigens in vitro can prime antigen-specific, MHC-restricted T cells in situ. [Published erratum appears in *1990 J Exp Med 172: 1275*]. J Exp Med. 1990; 172:631–640. [PubMed: 2373994]
2. Mullins DW, Bullock TN, Colella TA, Robila VV, Engelhard VH. Immune responses to the HLA-A*0201-restricted epitopes of tyrosinase and glycoprotein 100 enable control of melanoma outgrowth in HLA-A*0201-transgenic mice. J Immunol. 2001; 167:4853–4860. [PubMed: 11673489]
3. Mullins DW, Sheasley SL, Ream RM, Bullock TN, Fu YX, Engelhard VH. Route of immunization with peptide-pulsed dendritic cells controls the distribution of memory and effector T cells in

lymphoid tissues and determines the pattern of regional tumor control. J Exp Med. 2003; 198:1023–1034. [PubMed: 14530375]

4. Zarei S, Abraham S, Arrighi JF, Haller O, Calzascia T, Walker PR, Kundig TM, Hauser C, Piguet V. Lentiviral transduction of dendritic cells confers protective antiviral immunity in vivo. J Virol. 2004; 78:7843–7845. [PubMed: 15220461]
5. Lappin MB, Weiss JM, Delattre V, Mai B, Dittmar H, Maier C, Manke K, Grabbe S, Martin S, Simon JC. Analysis of mouse dendritic cell migration in vivo upon subcutaneous and intravenous injection. Immunology. 1999; 98:181–188. [PubMed: 10540216]
6. Eggert AA, Schreurs MW, Boerman OC, Oyen WJ, de Boer AJ, Punt CJ, Figdor CG, Adema GJ. Biodistribution and vaccine efficiency of murine dendritic cells are dependent on the route of administration. Cancer Res. 1999; 59:3340–3345. [PubMed: 10416590]
7. Morse MA, Coleman RE, Akabani G, Niehaus N, Coleman D, Lyerly HK. Migration of human dendritic cells after injection in patients with metastatic malignancies. Cancer Res. 1999; 59:56–58. [PubMed: 9892184]
8. Okada N, Tsujino M, Hagiwara Y, Tada A, Tamura Y, Mori K, Saito T, Nakagawa S, Mayumi T, Fujita T, Yamamoto A. Administration route-dependent vaccine efficiency of murine dendritic cells pulsed with antigens. Br J Cancer. 2001; 84:1564–1570. [PubMed: 11384109]
9. Olasz EB, Lang L, Seidel J, Green MV, Eckelman WC, Katz SI. Fluorine-18 labeled mouse bone marrow-derived dendritic cells can be detected in vivo by high resolution projection imaging. J Immunol Methods. 2002; 260:137–148. [PubMed: 11792384]
10. Stagg AJ, Kamm MA, Knight SC. Intestinal dendritic cells increase T cell expression of $\alpha_4\,\beta_7$ integrin. Eur J Immunol. 2002; 32:1445–1454. [PubMed: 11981833]
11. Johansson-Lindbom B, Svensson M, Wurbel MA, Malissen B, Marquez G, Agace W. Selective generation of gut tropic T cells in gut-associated lymphoid tissue (GALT): requirement for GALT dendritic cells and adjuvant. J Exp Med. 2003; 198:963–969. [PubMed: 12963696]
12. Mora JR, Bono MR, Manjunath N, Weninger W, Cavanagh LL, Rosemblatt M, von Andrian UH. Selective imprinting of gut-homing T cells by Peyer's patch dendritic cells. Nature. 2003; 424:88–93. [PubMed: 12840763]
13. Dudda JC, Lembo A, Bachtanian E, Huehn J, Siewert C, Hamann A, Kremmer E, Forster R, Martin SF. Dendritic cells govern induction and reprogramming of polarized tissue-selective homing receptor patterns of T cells: important roles for soluble factors and tissue microenvironments. Eur J Immunol. 2005; 35:1056–1065. [PubMed: 15739162]
14. Dudda JC, Simon JC, Martin S. Dendritic cell immunization route determines $CD8^+$ T cell trafficking to inflamed skin: role for tissue microenvironment and dendritic cells in establishment of T cell-homing subsets. J Immunol. 2004; 172:857–863. [PubMed: 14707056]
15. Mora JR, Cheng G, Picarella D, Briskin M, Buchanan N, von Andrian UH. Reciprocal and dynamic control of CD8 T cell homing by dendritic cells from skin- and gut-associated lymphoid tissues. J Exp Med. 2005; 201:303–316. [PubMed: 15642741]
16. Bullock TNJ, Colella TA, Engelhard VH. The density of peptides displayed by dendritic cells affects immune responses to human tyrosinase and gp100 in HLA-A2 transgenic mice. J Immunol. 2000; 164:2354–2361. [PubMed: 10679070]
17. Gallatin WM I, Weissman L, Butcher EC. A cell-surface molecule involved in organ-specific homing of lymphocytes. Nature. 1983; 304:30–34. [PubMed: 6866086]
18. Andrew DP, Berlin C, Honda S, Yoshino T, Hamann A, Holzmann B, Kilshaw PJ, Butcher EC. Distinct but overlapping epitopes are involved in $\alpha_4\beta_7$-mediated adhesion to vascular cell adhesion molecule-1, mucosal addressin-1, fibronectin, and lymphocyte aggregation. J Immunol. 1994; 153:3847–3861. [PubMed: 7523506]
19. Streeter PR, Berg EL, Rouse BT, Bargatze RF, Butcher EC. A tissue-specific endothelial cell molecule involved in lymphocyte homing. Nature. 1988; 331:41–46. [PubMed: 3340147]
20. Levelt CN, Mombaerts P, Wang B, Kohler H, Tonegawa S, Eichmann K, Terhorst C. Regulation of thymocyte development through CD3: functional dissociation between $p56^{lck}$ and $CD3\sigma$ in early thymic selection. Immunity. 1995; 3:215–222. [PubMed: 7648394]

21. Camerini V, Panwala C, Kronenberg M. Regional specialization of the mucosal immune system: intraepithelial lymphocytes of the large intestine have a different phenotype and function than those of the small intestine. J Immunol. 1993; 151:1765–1776. [PubMed: 8345182]
22. Cruise MW, Melief HM, Lukens J, Soguero C, Hahn YS. Increased Fas ligand expression of $CD4^+$ T cells by HCV core induces T cell-dependent hepatic inflammation. J Leukocyte Biol. 2005; 78:412–425. [PubMed: 15894587]
23. Shurin MR, Pandharipande PP, Zorina TD, Haluszczak C, Subbotin VM, Hunter O, Brumfield A, Storkus WJ, Maraskovsky E, Lotze MT. FLT3 ligand induces the generation of functionally active dendritic cells in mice. Cell Immunol. 1997; 179:174–184. [PubMed: 9268501]
24. Brinkmann V, Lynch KR. FTY720: targeting G-protein-coupled receptors for sphingosine 1-phosphate in transplantation and autoimmunity. Curr Opin Immunol. 2002; 14:569–575. [PubMed: 12183155]
25. Hamann A, Andrew DP, Jablonski-Westrich D, Holzmann B, Butcher EC. Role of α_4-integrins in lymphocyte homing to mucosal tissues in vivo. J Immunol. 1994; 152:3282–3293. [PubMed: 7511642]
26. Clarke SR, Barnden M, Kurts C, Carbone FR, Miller JF, Heath WR. Characterization of the ovalbumin-specific TCR transgenic line OT-I: MHC elements for positive and negative selection. Immunol Cell Biol. 2000; 78:110–117. [PubMed: 10762410]
27. Tilney NL. Patterns of lymphatic drainage in the adult laboratory rat. J Anat. 1971; 109:369–383. [PubMed: 5153800]
28. Abu-Hijleh MF, Habbal OA, Moqattash ST. The role of the diaphragm in lymphatic absorption from the peritoneal cavity. J Anat. 1995; 186:453–467. [PubMed: 7559120]
29. Andrade W, Johnston MG, Hay JB. The exit of lymphocytes and RBCs from the peritoneal cavity of sheep. Immunobiology. 1996; 195:77–90. [PubMed: 8852602]
30. Campbell DJ, Butcher EC. Rapid acquisition of tissue-specific homing phenotypes by $CD4^+$ T cells activated in cutaneous or mucosal lymphoid tissues. J Exp Med. 2002; 195:135–141. [PubMed: 11781372]
31. Calzascia T, Masson F, Di Berardino-Besson W, Contassot E, Wilmotte R, Aurrand-Lions M, Ruegg C, Dietrich PY, Walker PR. Homing phenotypes of tumor-specific CD8 T cells are predetermined at the tumor site by crosspresenting APCs. Immunity. 2005; 22:175–184. [PubMed: 15723806]
32. Dudda JC, Martin SF. Tissue targeting of T cells by DCs and microenvironments. Trends Immunol. 2004; 25:417–421. [PubMed: 15275640]
33. Iwata M, Hirakiyama A, Eshima Y, Kagechika H, Kato C, Song SY. Retinoic acid imprints gut-homing specificity on T cells. Immunity. 2004; 21:527–538. [PubMed: 15485630]
34. Lambrecht BN, Pauwels RA, de St Groth BF. Induction of rapid T cell activation, division, and recirculation by intratracheal injection of dendritic cells in a TCR transgenic model. J Immunol. 2000; 164:2937–2946. [PubMed: 10706680]
35. Lawrence CW, Braciale TJ. Activation, differentiation, and migration of naive virus-specific $CD8^+$ T cells during pulmonary influenza virus infection. J Immunol. 2004; 173:1209–1218. [PubMed: 15240712]
36. Kraal G, Schornagel K, Streeter PR, Holzmann B, Butcher EC. Expression of the mucosal vascular addressin, MAdCAM-1, on sinus-lining cells in the spleen. Am J Pathol. 1995; 147:763–771. [PubMed: 7677187]
37. Nolte MA, Hamann A, Kraal G, Mebius RE. The strict regulation of lymphocyte migration to splenic white pulp does not involve common homing receptors. Immunology. 2002; 106:299–307. [PubMed: 12100717]
38. Xie H, Lim YC, Luscinskas FW, Lichtman AH. Acquisition of selectin binding and peripheral homing properties by $CD4^+$ and $CD8^+$ T cells. J Exp Med. 1999; 189:1765–1776. [PubMed: 10359580]
39. Thoma S, Bonhagen K, Vestweber D, Hamann A, Reimann J. Expression of selectin-binding epitopes and cytokines by $CD4^+$ T cells repopulating *scid* mice with colitis. Eur J Immunol. 1998; 28:1785–1797. [PubMed: 9645359]

40. Schneck J, Munitz T, Coligan JE, Maloy WL, Margulies DH, Singer A. Inhibition of allorecognition by an H-2Kb-derived peptide is evidence for a T-cell binding region on a major histocompatibility complex molecule. Proc Natl Acad Sci USA. 1989; 86:8516–8520. [PubMed: 2813409]

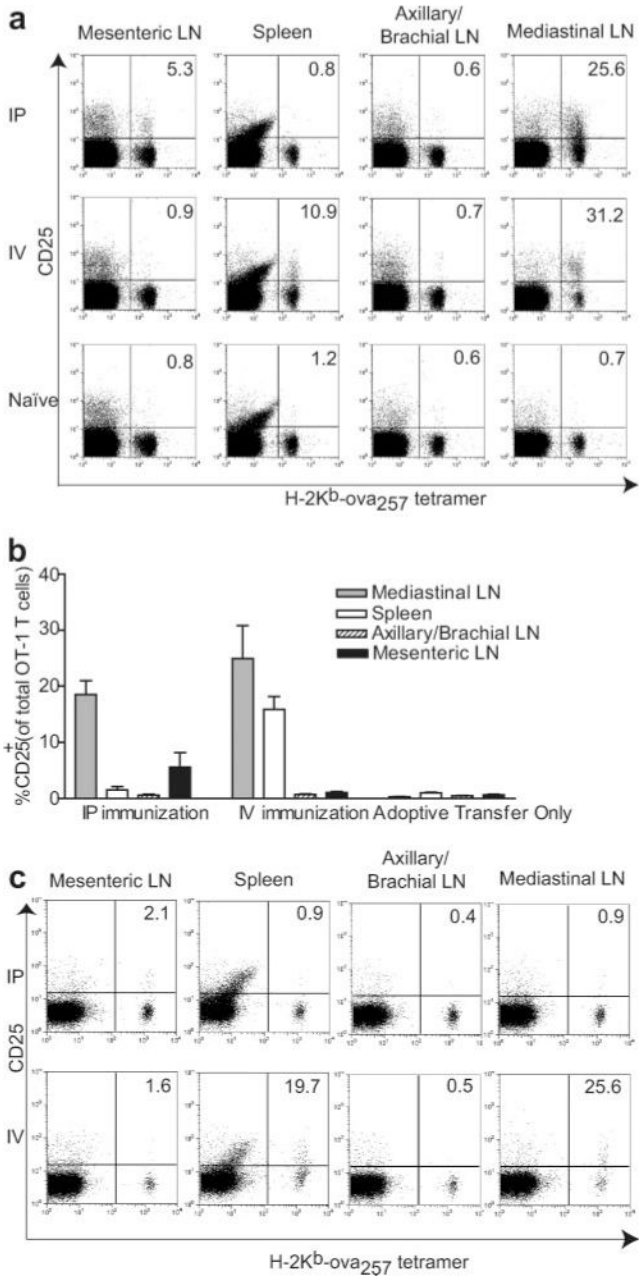

FIGURE 1.

OT-1 cell activation is differentially localized following i.v. or i.p. injection of CD40L-activated OVA_{257}-pulsed BMDC. *a*, Mice that had been adoptively transferred with CD8-enriched OT-1 cells were immunized, and lymphoid organs were harvested 22 h later for flow cytometry. OT-1 cells were identified by staining for CD8 and H-$2K^b$-OVA_{257}-tetramer, and activation was determined by CD25 expression. Representative data from an individual experiment. Dot plots are gated on $CD8^+$ lymphocytes, and numbers represent the percentage of H-$2K^b$-OVA_{257}-$tetramer^+$ cells that are $CD25^+$. *b*, Aggregate data from six to nine mice in each group (±SEM) analyzed in six independent experiments. *c*, Mice were immunized with CD40L-activated OVA_{257}-pulsed BMDC i.v. or i.p. CD8-enriched OT-1

cells were then adoptively transferred 48 h after BMDC injection. Lymphoid organs were harvested 24 h after T cell transfer and stained for flow cytometry, as described above. Data are individual animals from one experiment representative of four mice in immunized groups and two mice in adoptive transfer only group in two independent experiments.

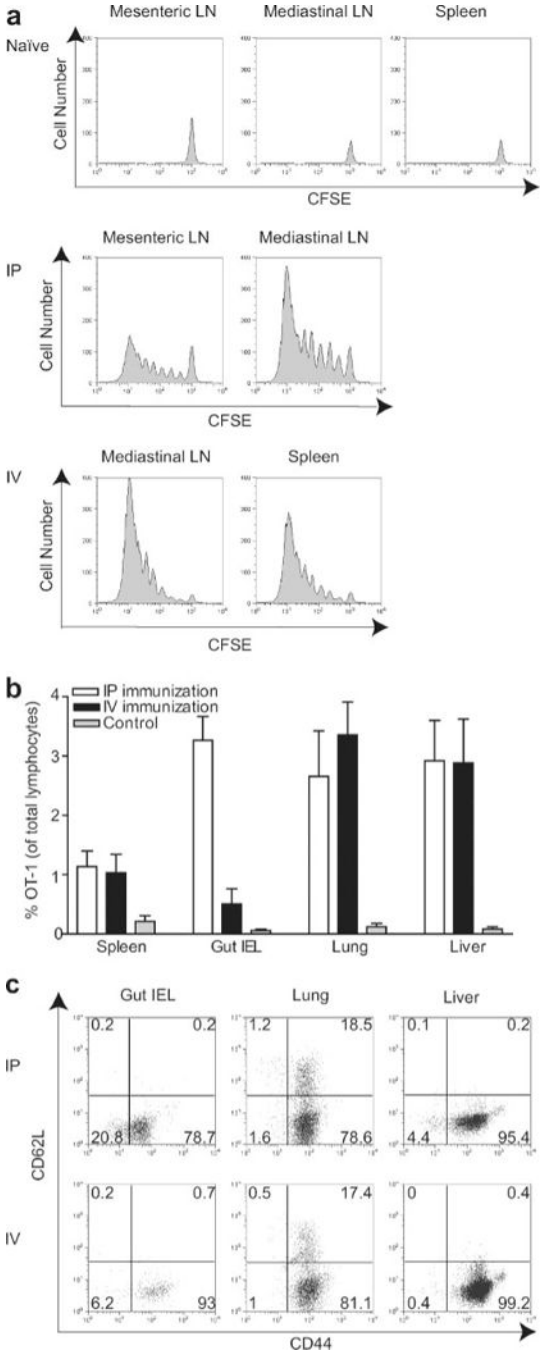

FIGURE 2.

Activated OT-1 cells proliferate in all priming compartments, but distribution in peripheral tissues is dependent on route of BMDC immunization. *a*, Mice that had been adoptively transferred with CD8-enriched OT-1 cells were immunized, and lymphoid organs representing priming compartments defined in Fig. 1 were harvested 3 days later for flow cytometry. Histograms are gated on Thy1.2$^+$ lymphocytes. *b* and *c*, Mice that had been adoptively transferred with 1×10^6 CD8-enriched OT-1 cells were immunized with BMDC, and lymphocytes were isolated from the indicated peripheral tissues 6 days later. OT-1 cells

were identified by Thy1.2 or CD8 and H-2K^{b}-OVA$_{257}$-tetramer staining. *b*, Data are mean values pooled from six mice per condition (±SEM) analyzed in five independent experiments. *c*, Representative dot plots from individual mice.

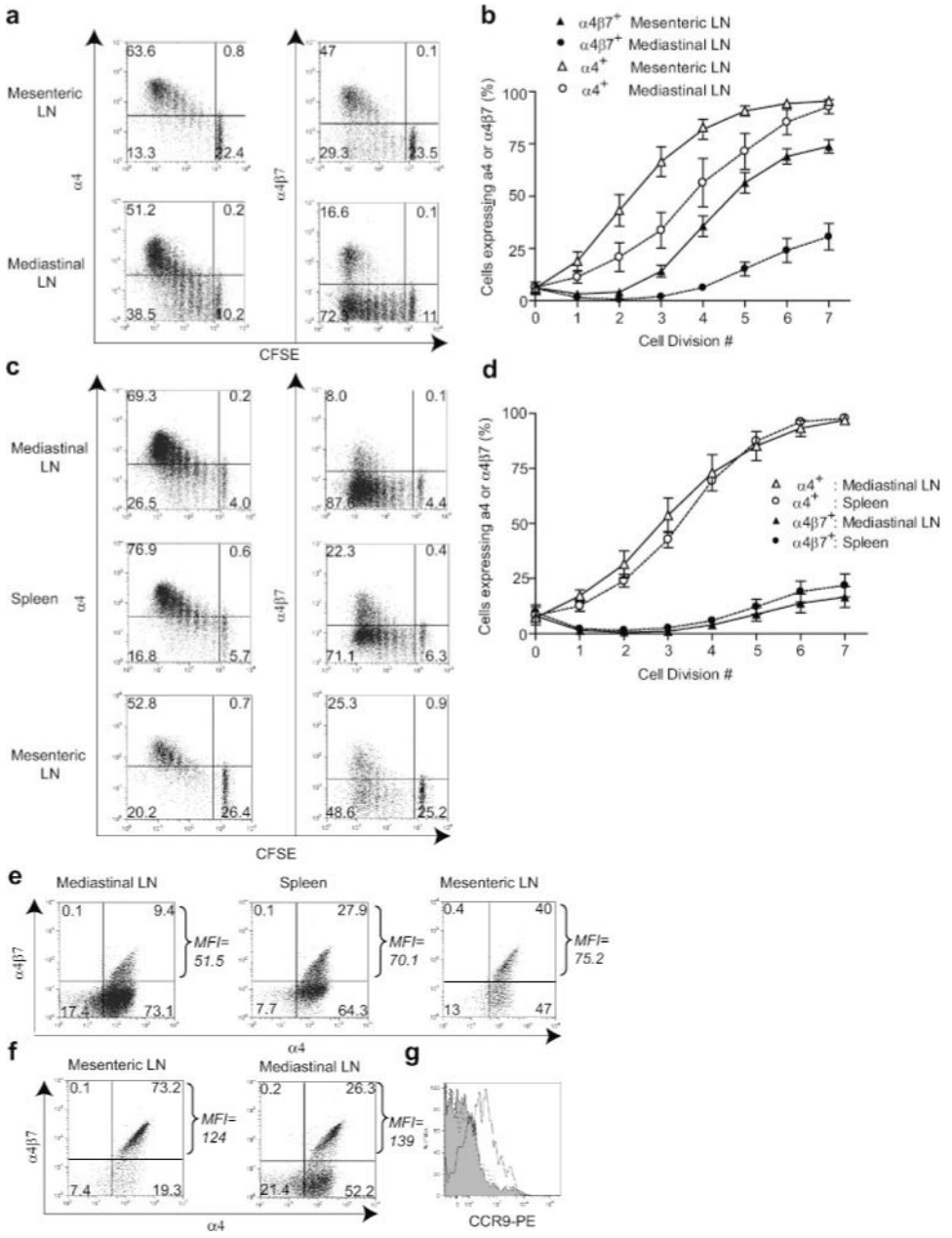

FIGURE 3.

Kinetics, level, and type of α_4 integrin expression differs in priming compartments after BMDC immunization. Mice that had been adoptively transferred with CD8-enriched OT-1 cells were immunized with BMDC by i.p. (*a*, *b*, *f*, and *g*) or i.v. (*c*, *d*, *e*, and *g*) routes, and lymphoid organs representing priming compartments defined in Fig. 1 were harvested 3 days later for flow cytometry. *a* and *c*, Representative data from individual mice. *b* and *d*, Percentage of OT-1 cells that were α_4^+ or $\alpha_4\beta_7^+$ at each cell division based on CFSE dilution. Data are mean values from five to six mice (±SEM) pooled from four to five independent experiments. *e* and *f*, Integrin expression on extensively divided OT-1 cells. Dot plots are on Thy1.2$^+$ lymphocytes that had undergone five or more cell divisions as determined by CFSE dilution. MFI of $\alpha_4\beta_7$ staining in *upper right quadrant* is indicated for

each dot plot. *g*, CCR9 expression on $\alpha_4\beta_7^+$ divided OT-1 cells from the mesenteric LN after i.p. immunization (open), mediastinal LN after i.v. immunization (shaded), and mesenteric LN with no immunization (dotted).

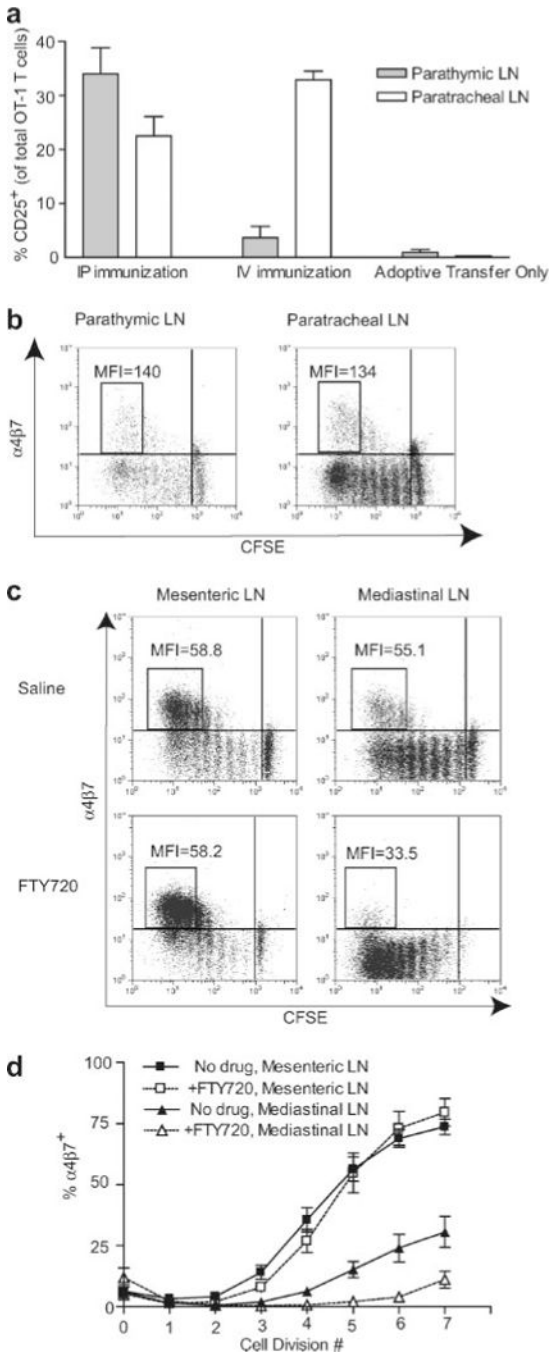

FIGURE 4.

The $\alpha_4\beta_7^{high}$ subpopulation of activated OT-1 cells in mediastinal LN after i.p. immunization originates in mesenteric LN. *a*, Mice that had been adoptively transferred with CD8-enriched OT-1 cells were immunized i.p. with BMDC, and the indicated LN were harvested 22 h or 3 days (40) later. OT-1 cells were identified by gating on $CD8^+H\text{-}2K^b\text{-}OVA_{257}\text{-tetramer}^+$ lymphocytes. *a*, OT-1 cell activation in separated components of the mediastinal LN. Data are mean values from five mice in immunized groups and three mice in adoptive transfer only group (±SEM). One of three independent experiments is shown. *b*,

$\alpha_4\beta_7$ expression on activated OT-1 cells in parathymic and paratracheal LN. MFI values refer to $\alpha_4\beta_7$ staining of cell populations in boxes. Data are representative of eight mice in two independent experiments. *c*, Effect of in vivo administration of FTY720 on $\alpha_4\beta_7$ expression on activated OT-1 cells in priming compartments. MFI values refer to $\alpha_4\beta_7$ staining of cell populations in boxes. *d*, Percentage of OT-1 cells that were $\alpha_4\beta_7^+$ at each cell division based on CFSE dilution. Data are mean values from six mice (±SEM) analyzed in three independent experiments. There was no significant difference between mesenteric LN between FTY720-treated and control mice ($p = 0.828$), but differences in mediastinal LN were significantly different ($p < 0.001$) as determined by two-way ANOVA.

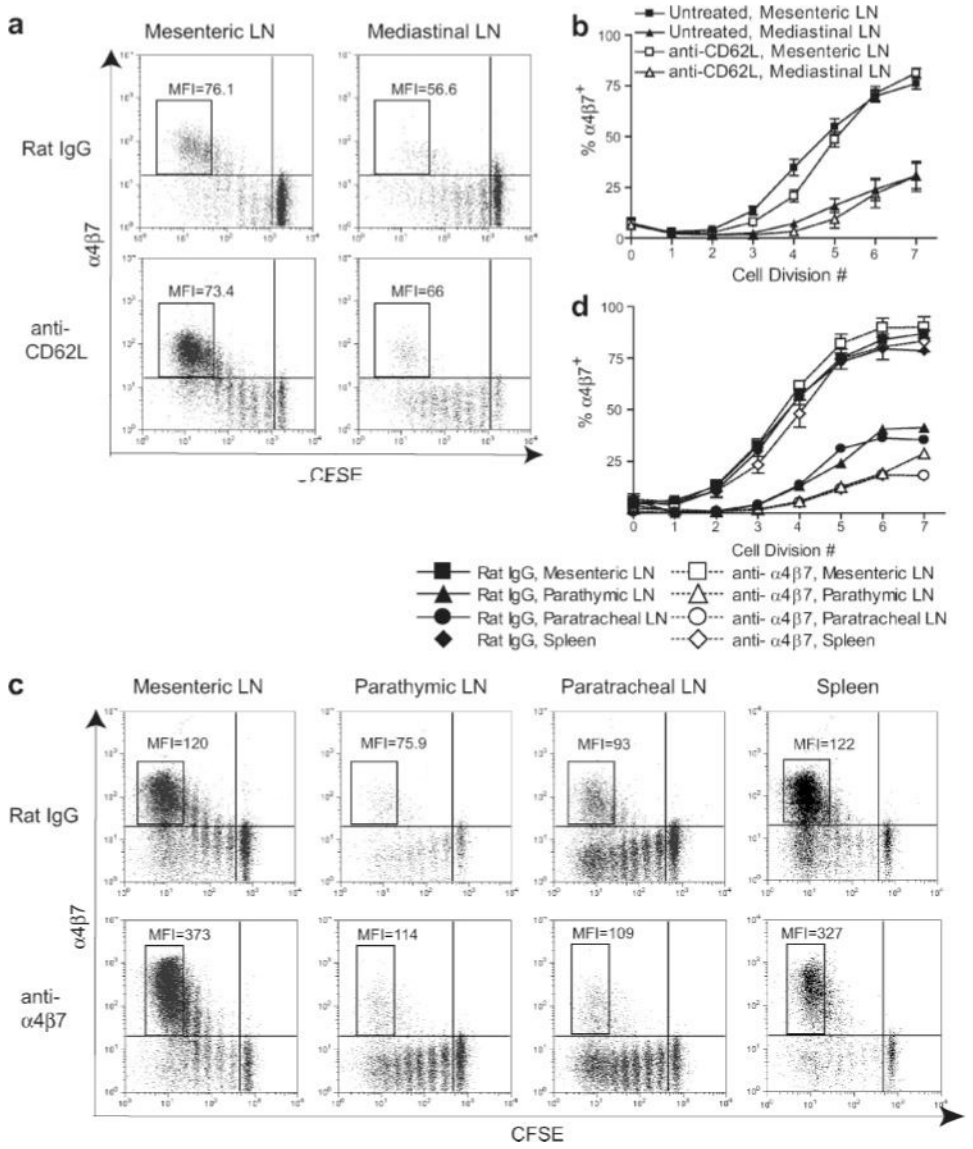

FIGURE 5.

$\alpha_4\beta_7^{high}$ OT-1 cells are activated in mesenteric LN and redistribute into mediastinal LN. Mice were adoptively transferred with CFSE-labeled OT-1 cells before i.p. immunization. Ab treatment was initiated 6 h (anti-CD62L) or 24 h (anti-$\alpha_4\beta_7$) after BMDC injection and continued until harvest at 72 h. Dot plots are gated on $CD8^+$H-$2K^b$-OVA_{257}-tetramer$^+$ lymphocytes. MFI values refer to $\alpha_4\beta_7$ staining of cell populations in boxes. *a* and *b*, Effects of blockade with anti-CD62L. *a*, Data from individual mice representative of eight mice treated with each reagent in three independent experiments. *b*, Data are mean values (±SEM) from eight mice per group analyzed in three independent experiments. *c* and *d*, Effects of blockade with anti-$\alpha_4\beta_7$. *c*, Data from mesenteric LN and spleen of individual mice and parathymic and paratracheal LN pooled from two mice. Representative of eight mice treated with each reagent in four independent experiments. Because of the presence of in vivo bound anti-$\alpha_4\beta_7$ Ab on OT-1 cells in anti-$\alpha_4\beta_7$-treated mice, these cells were stained with PE anti-rat IgG, leading to an elevated MFI. Cells from mice treated with rat IgG were

stained normally, as described in *Materials and Methods*. *d*, Data are mean values (±SEM) from two mice per group, except parathymic and paratracheal LN, which were values obtained from pooling samples from two mice. Data are representative of four independent experiments.

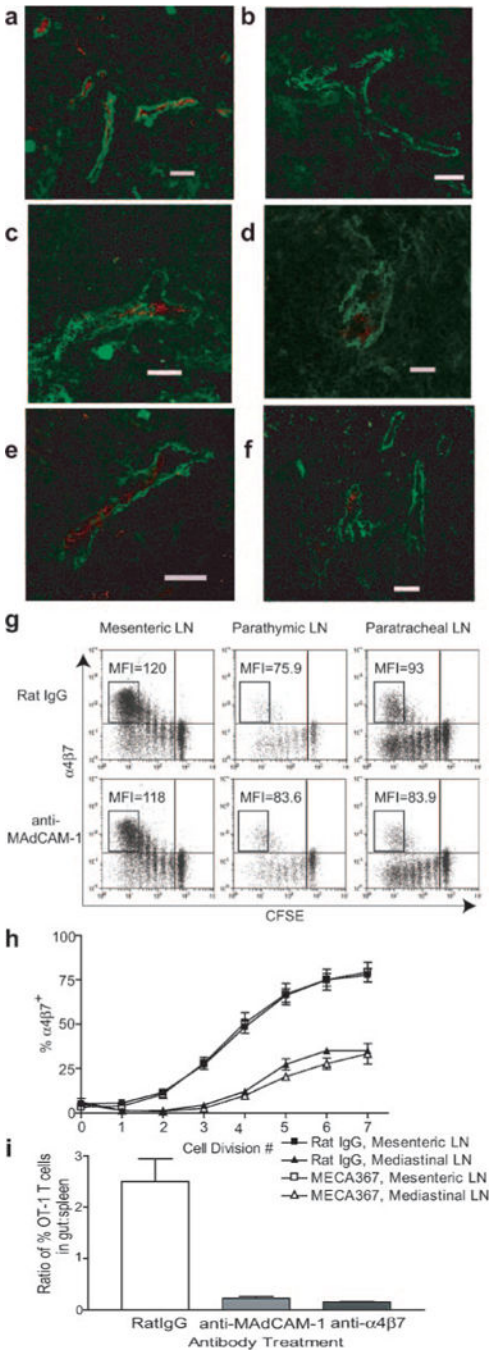

FIGURE 6.

MAdCAM-1 expression and its role in the entry of $\alpha_4\beta_7^{high}$ cells into mediastinal LN. *a–f*, Expression of MAdCAM-1 in mesenteric (*a*), brachial (*b*), parathymic (*c*), and paratracheal (*d*) LN in naive mice, as well as parathymic (*e*) and paratracheal (*f*) LN of i.p. immunized mice. MAdCAM-1 staining is red, and smooth muscle α-actin staining (to delineate HEV) is green. Scale bar equals 50 μm. *g* and *h*, Entry of $\alpha_4\beta_7^{high}$ cells into mediastinal LN is MAdCAM-1 independent. Mice were adoptively transferred with CFSE-labeled OT-1 cells before i.p. immunization. Ab treatment was initiated 24 h after BMDC injection and

continued until harvest at 72 h. *g*, Dot plots are gated on $CD8^+H\text{-}2K^b\text{-}OVA_{257}\text{-}tetramer^+$ lymphocytes. MFI values refer to $\alpha_4\beta_7$ staining of cell populations in boxes. *h*, Percentage of OT-1 cells that were $\alpha_4\beta_7^+$ at each cell division based on CFSE dilution. Data are mean values from six to nine mice (±SEM) analyzed in three independent experiments. *i*, Mice were adoptively transferred with CFSE-labeled OT-1 cells before i.p. immunization. Ab treatment was initiated 24 h after BMDC injection and continued every 24 h. Tissues were harvested 3 days after BMDC injection. Intraepithelial lymphocytes were recovered, as described in *Materials and Methods*. Data are mean values (±SEM) from three to four mice analyzed in three independent experiments.

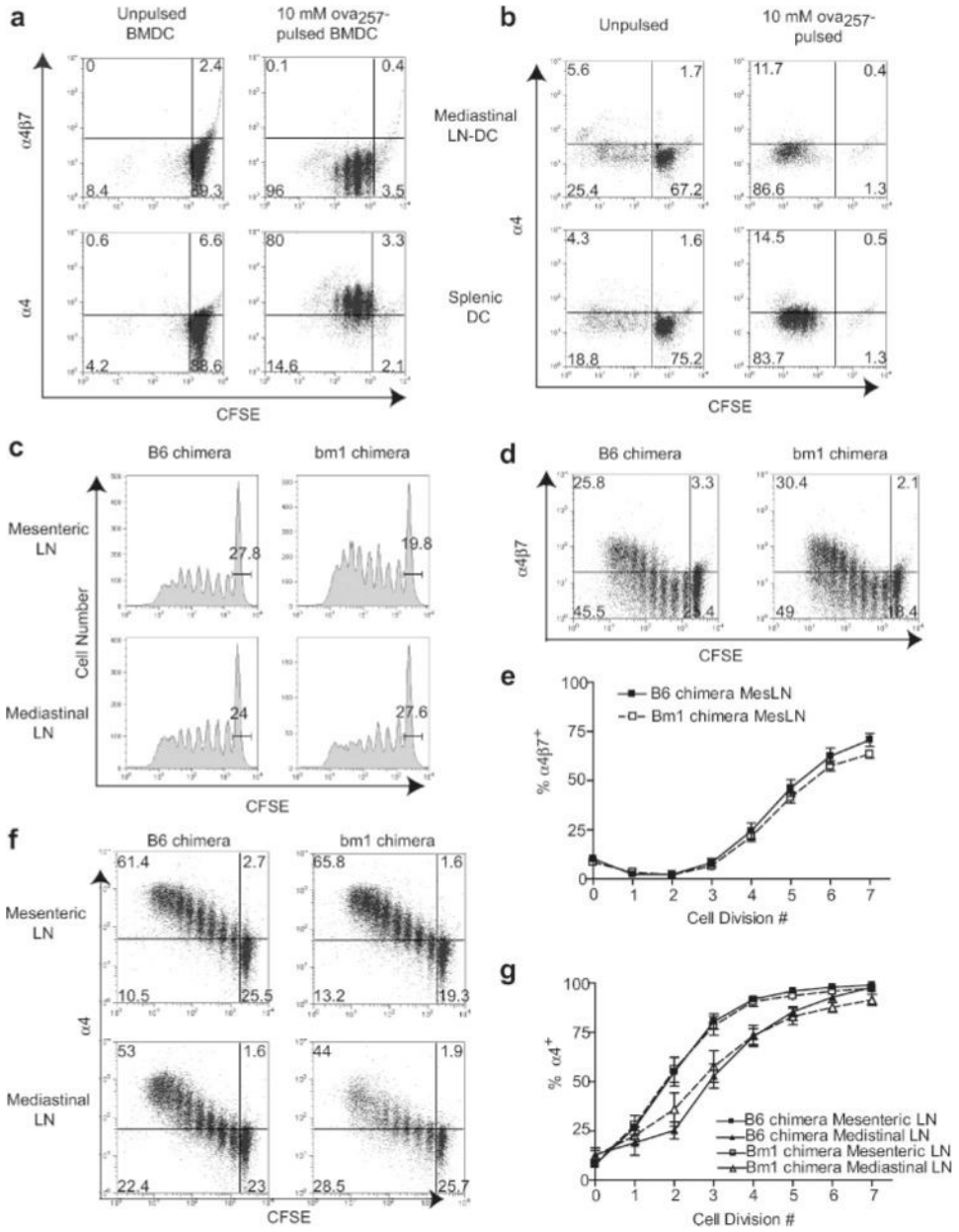

FIGURE 7.

Roles of BMDC and endogenous DC in imprinting of α_4 integrin expression on activated OT-1 cells. *a* and *b*, CFSE-labeled, CD8-enriched OT-1 cells were cultured in vitro for 4 days with unpulsed or 10 μM OVA_{257}-pulsed CD40L-activated BMDC (*a*) or DC enriched from mediastinal LN or spleen (*b*) from *fms*-like tyrosine kinase-3 ligand-treated mice. Dot plots are gated on $CD8^+$ (*a*) or $Thy1.2^+$ (*b*) lymphocytes. Data are representative of three independent experiments. *c*–*g*, Lethally irradiated B6 mice were reconstituted with bone marrow from either bm1 or B6 mice. At least 10 wk after bone marrow transplant, these bone marrow were adoptively transferred with CFSE-labeled, CD8-enriched OT-1 cells, and then immunized i.p. with CD40L-activated OVA_{257}-pulsed BMDC. Lymphoid organs were collected 3 days after immunization. *c*, OT-1 cell proliferative responses in priming

compartments of bm1 and B6 chimeras. Histograms are gated on $CD8^+$H-$2K^b$-OVA_{257}-tetramer$^+$ lymphocytes. Values are percentage of CFSE undiluted of total OT-1 cells. *d*, Expression of $\alpha_4\beta_7$ on OT-1 cells in the mesenteric LN of bm1 and B6 chimeras. Dot plots are gated on $CD8^+$H-$2K^b$-OVA_{257}-tetramer$^+$ lymphocytes. *e*, Percentage of OT-1 cells that were $\alpha_4\beta_7^+$ at each cell division in the mesenteric LN as determined by CFSE dilution. Data are mean values (±SEM) from five bm1 chimeras and four B6 chimeras analyzed in three independent experiments. *f*, Expression of α_4 on OT-1 cells in priming compartments of bm1 and B6 chimeras. Dot plots are gated on $CD8^+$H-$2K^b$-OVA_{257}-tetramer$^+$ lymphocytes. *g*, Percentage of OT-1 cells that were α_4^+ at each cell division in priming compartments as determined by CFSE dilution. Data are mean values (±SEM) from five bm1 chimeras and four B6 chimeras analyzed in three independent experiments.